

# Development of lightweight construction blocks by alkaline activation of BOF slag

N.T. Sithole<sup>1</sup>, F Okonta<sup>2</sup>, F. Ntuli<sup>1</sup>

<sup>1</sup> University of Johannesburg, Department of Chemical Engineering, P.O. Box 17011, Doornfontein 2088, South Africa, \* corresponding author email address:nastassias@uj.ac.za, fntuli@uj.ac.za

<sup>2</sup>Department of Civil Engineering Science, University of Johannesburg, P O Box 524, Auckland Park, 2006, Johannesburg, South Africa, email address:fokonta@uj.ac.za

---

## Abstract

Large quantities of basic oxygen furnace (BOFS) are dumped in landfills of which the available land for land-filling of large quantities of waste is reducing all over the world. It is therefore important to develop processes which beneficiates solid waste; BOF slag specifically. The present study attempts to investigate the potential to synthesize BOF slag based light weight construction blocks. The effects of several factors on the UCS of BOF slag based light weight construction blocks (LWCB) was also investigated. The test variables were molarities of sodium hydroxide (NaOH) (5 M, 10 M and 15 M); the solid to liquid ratio (20 %, 25 % and 30 %); the sodium silicate (Na<sub>2</sub>SiO<sub>3</sub>) to NaOH ratio (0.5:1, 1:1, 1.5:1, 2:1, 2.5:1 and 3:1); the curing temperature (40°C, 80°C and 100°C). It was found that optimum synthesis conditions were 5M NaOH, 80°C and 1:1 Sodium Silicate: NaOH ratio. The LWCB composite met the minimum requirements for ASTM C34-13, C129-14a and South African standard (SANS227: 2007).

Keywords: Basic oxygen furnace slag, lightweight construction block, alkaline activation, geopolymer, porosity.

## 1.1. Introduction

Ordinary Portland Cement (OPC) is the most commonly used binder in the construction industry. The manufacturing of OPC presents so many problems. It consumes significant amount of natural materials and energy; however Africa's energy crisis continues to grow. It was reported that the production of 1 ton of OPC consumes about 1.5 tons of limestone which approximately emits 1 ton of carbon dioxide (CO<sub>2</sub>) to the atmosphere (Pereira et al., 2015 and Zhang et al., 2011). The South African cement industry is one of the major consumers of energy (thermal and electricity)

31 in the country and accounts for 8 % of the total CO<sub>2</sub> emission from industries (Ohanyere, 2013;  
32 Pelsler, 2017). South Africa is responsible for nearly half the CO<sub>2</sub> emissions for the entire continent  
33 of Africa. Worldwide, the cement industry accounts for 7% of all CO<sub>2</sub> generated (Bernard et al.,  
34 2017; Bar and Azam, 2017). In line with South African government commitment to find a  
35 sustainable carbon low path in the construction of infrastructure to mitigate greenhouse gas  
36 emissions, especially CO<sub>2</sub>; it is therefore of great national importance to find an alternative binder  
37 to reduce the utilization of Portland cement (Falayi et al., 2017).

38 A feasible alternative is alkaline activation of industrial by-products like fly ash, ground granulated  
39 blast furnace slag, steel slag, copper slag generated from various industries as an alternative to  
40 OPC. An estimate of about 2.4 million tons of BOF slag is produced annually in South Africa of  
41 which about 5 % is recycled the remainder being disposed in heaps (Sithole, 2016). Compared to  
42 other countries like China and USA which produces thrice the amount of BOF slag; only 22% is  
43 utilized. The utilization of BOF slag in Africa is still limited and it is still particularly low in South  
44 Africa. According to Kambole et al., 2017 one of the resulting factors for limited utilization of  
45 BOF slag is that there are very limited studies on the utilization of BOF slag in Africa, specifically  
46 in Southern Africa. This may partly explains why most Southern African construction  
47 specifications do not cater for slags, resulting in the limited use of this recyclable material resource  
48 in construction. There is a need for Southern Africa to consider increased use of BOF slag in  
49 construction (Kambole et al., 2017).

50 The use of BOF slag as a cementing material to replace Portland cement and as a hydraulic binder  
51 is well documented (Belhadj et al., 2014; Wang and Yang 2010; Brand et al., 2015; Ren et al.,  
52 2017). In addition the use of BOF slag aggregates for road construction is well documented in  
53 literature (Chen et al., 2016; Haritonovs et al., 2013; Motz and Geiseler, 2001, Egesi, 2012; Xue,  
54 2006; Taherkhani, 2015; Ioannou et al., 2013). Some researchers (Belhadj et al., 2014; Brand et  
55 al., 2015; Taherkhani, 2015; Ren et al., 2017) reported that BOF slag is an expansive material due  
56 to the presence of free lime in BOF slag, and thus it cannot be used for construction works.  
57 However, it has also been reported that slag expansion could be avoided if the slag particle sizes  
58 of limited to 13.2 mm for construction work (Ameri et al., 2013; Yüksel, 2017). Furthermore BOF  
59 slag expansion might be dependent on the type of minerology and chemical nature. They would  
60 differ as per manufacturing processes and the source of the raw material. It is noted that also

61 investigations and studies regarding the production of BOF slag based lightweight geopolymers  
 62 are scarce and limited. The present study attempts to fully beneficiate BOF slag by development  
 63 of light weight construction blocks. The utilization of BOF slag in making LWCB is rare and not  
 64 well documented in literature. LWCB are construction composites with a density of less than 1680  
 65 kg/m<sup>3</sup> and a minimum unconfined compressive strength (UCS) of 4.1 MPa (ASTM C129-14a).  
 66 The advantage of LWCB is that it reduces the dead load of a building (Falayi et al., 2017).

## 67 2. Methodology

### 69 2.1. Materials and Methods

70 BOFS was obtained from ArcelorMittal South Africa. Sodium silicate solution was supplied by  
 71 Sigma Aldrich South Africa. Sodium hydroxide was supplied by a chemical company South  
 72 Africa. Table 1 shows the chemical and geotechnical properties of BOF slag.

73 **Table 1: Chemical and geotechnical properties of BOF slag**

Parameter	BOF slag
pH	12.4
Specific gravity	3.25
% CaO	51.81
% Al <sub>2</sub> O <sub>3</sub>	3.5
% SiO <sub>2</sub>	7.7
% MnO	4.188
% Fe <sub>2</sub> O <sub>3</sub>	27.58
% Gravel	0
% Sand	77.92
% Fine	11.12
% Silt	10.96
Liquid limit	76
Plastic limit	non plastic
Shrinkage limit	non shrinking
MDD (kg/m <sup>3</sup> )	2265
OMC (%)	10.58

74  
 75 The chemical and geotechnical characterization was performed prior to alkaline activation to better  
 76 understand the properties of BOF slag. The specific gravity of basic oxygen furnace slag was found  
 77 to be 3.25. This specific gravity is greater than the specific gravity of natural inorganic soils which

78 typically ranges between of 2.6 to 2.9. This is attributed to the high  $\text{Fe}_2\text{O}_3$  content in BOF slag.  
79 The main constituents of BOF slag are calcium oxide ( $\text{CaO}$ ), iron oxide ( $\text{Fe}_2\text{O}_3$ ), silicon dioxide  
80 ( $\text{SiO}_2$ ), and magnesium oxide ( $\text{MgO}$ ). The  $\text{Fe}_2\text{O}_3$  content for this sample is higher than those of  
81 most BOF steel slags reported in literature (Yildirim et al., 2015). However, according to Shen et  
82 al. (2009), the  $\text{Fe}_2\text{O}_3$  content of BOF steel slag can be as high as up to 38% depending on the  
83 amount of oxidized iron that cannot be recovered during the conversion process of molten iron to  
84 steel. BOFS has the lowest  $\text{SiO}_2$ ,  $\text{Al}_2\text{O}_3$ , content compared to other aluminosilicate sources (fly  
85 ash, metakaolin, granulated blast furnace slag and mine tailings) which have been used to achieve  
86 an efficient geopolymer synthesis.  $\text{SiO}_2$  and  $\text{Al}_2\text{O}_3$ , contents of BOF slag are respectively 5-7 times  
87 and 6-8 times lower than those of fly ash, metakaolin and GBFS. In this study the problem of low  
88  $\text{SiO}_2$  and  $\text{Al}_2\text{O}_3$  in BOF slag is addressed through  $\text{Na}_2\text{SiO}_4$  addition. The addition of sodium silicate  
89 provided  $\text{Si}^+$  ions as a secondary source and the  $\text{Na}^+$  ions played a vital role in the formation of  
90 geopolymer by acting as charge balancing ions; and also help to enhance strength development  
91 (Part el al., 2015). It is also noticeable that BOF slag compositions are similar to those of clinker.  
92 These compositions revealed that BOF slag exhibits cementitious properties. It has been reported  
93 by several researchers that BOF slag is a weak Portland cement clinker (Shi 2002), due to the fact  
94 that  $\text{C}_3\text{S}$  content in BOF slag is very low and sometimes the  $\text{C}_3\text{S}$  is not in the BOF slag sample at  
95 all (Tsakiridis et al., 2008). BOF slag sample used in this study reveals that  $\text{C}_3\text{S}$  is present since  
96 the  $\text{CaO/Si}$  ratio is greater than 2.7 (Shi 2002). The  $\text{C}_3\text{S}$  is well known to be responsible for  
97 hardening, initial setting and early strength development of Portland cement concrete (Reddy et  
98 al., 2006). Additionally the high Ca content in BOF slag played a role in forming C-H-S gel during  
99 alkaline activation. The formation of C-S-H gel may help to make a dense and homogeneous  
100 geopolymer paste (Kumar et al., 2009). Based on the properties of BOF slag revealed by XRF  
101 analysis; this study attempted to investigate the feasibility of synthesizing LWCB from BOF slag  
102 via alkaline activation. The low Atterberg limits could be classified as a sandy material with non-  
103 plastic and non-shrinking behavior.

## 104 **2.2. Equipments**

105  
106 X-Ray fluorescence (XRF; Rigaku ZSX Primus II) was used to determine the chemical  
107 composition of the geopolymer. FTIR (Thermo scientific IS10) was used to characterize of BOF  
108 slag before and after the alkaline activation. XRD was used to identify the mineralogical phases  
109 on the BOFS before and after alkaline activation. The BOFS morphology was captured using a

110 Scanning Electron Microscopy (SEM; Tescan Vega 3 XMU 1) to investigate the micro-structure  
 111 of the BOF slag before and after alkaline activation.

112 **2.3. Geopolymer paste preparation**

113  
 114 1100 kg BOFS and NaOH solution varied from 5 to 15 M as shown in Table 2 were mixed keeping  
 115 the S/L ratio fixed. After forming a workable slurry, the slurry was poured into a 100 x 100 x 100  
 116 mm<sup>3</sup> mould. The cast sample was allowed to set and was removed from the mould when it was  
 117 stiff enough for demolding. The hardened samples were then cured at 80°C until they were dry.  
 118 Molding was done in triplicate.

119  
 120

**Table 2 Mix ratio of NaOH and BOFS**

<i>% BOFS</i>	<i>NaOH Concentration (M)</i>	<i>Solid/Liquid ratio</i>
100	5	30
100	10	30
100	15	30

121

122 **2.3.1. The effect of solid/liquid ratio**

123

124 1100 kg of BOFS was mixed with 5 M NaOH and cured under different solid/ liquid ratios and  
 125 curing regime as shown in Table 3.

126

**Table 3 Solid/ liquid ratio variation**

<i>% BOFS</i>	<i>NaOH Concentration (M)</i>	<i>Solid/Liquid ratio(%)</i>	<i>Na<sub>2</sub>SiO<sub>3</sub>/NaOH ratio</i>
100	5	20	2:1
100	5	25	2:1
100	5	30	2:1

127

128 **2.3.2. The effect of temperature**

129

130 The BOFS was mixed with 5M NaOH and cured under different temperatures and the curing  
 131 regime as shown in Table 4

132

**Table 4 Curing temperature variation**

<i>% BOFS</i>	<i>NaOH Concentration (M)</i>	<i>Solid/Liquid ratio (%)</i>	<i>Na<sub>2</sub>SiO<sub>3</sub>/NaOH ratio</i>	<i>Temperature (°C)</i>
100	5	20	2:1	40
100	5	20	2:1	80
100	5	20	2:1	100

133

134 **2.3.3. The effect of Na<sub>2</sub>SiO<sub>3</sub>/NaOH ratio**

135 The BOFS was mixed with Na<sub>2</sub>SiO<sub>3</sub> and NaOH under different ratios as shown in Table 5.

136 **Table 5. Variation of Na<sub>2</sub>SiO<sub>3</sub>/ NaOH ratio**

<i>% BOFS</i>	<i>NaOH Concentration (M)</i>	<i>Solid/Liquid ratio (%)</i>	<i>Na<sub>2</sub>SiO<sub>3</sub>/NaOH ratio</i>	<i>Temperature (°C)</i>
100	5	20	0.5:1	80
100	5	20	1:1	80
100	5	20	1.5:1	80
100	5	20	2:1	80
100	5	20	2.5:1	80

137

138 **2.4. Open porosity**

139

140 The specimens were weighed after curing then they were immersed in a water bath for 24 h. 24 h had been  
141 determined as the time when an increase in mass of wet specimen was less than 1%. After 24 h the  
142 specimens were removed from water and were wiped using a soft cloth to remove any visible water. The  
143 wet specimens were weighed within 5 min after being removed from the water. Open porosity, *f*, was then  
144 calculated using equation (1) as follows (ASTM C373 – 14):

145

146 
$$f = \frac{W_s - W_d}{V\alpha}$$

147 where *W<sub>s</sub>* is the mass of the soaked specimen, *W<sub>d</sub>* was the mass of the dry specimen, *V* was the  
148 volume of the specimen and *α* was the density of water.

149 **2.5. Wet compressive strength**

150

151 The specimen was weighed after curing then, it was soaked in water for 24 h. After 24 h the  
152 specimen was removed from the water and wiped with a soft cloth then weighed. Immediately  
153 after weighing the wet specimen was then tested for UCS. A similar procedure was also used to  
154 assess whether the LWCB is expansive.

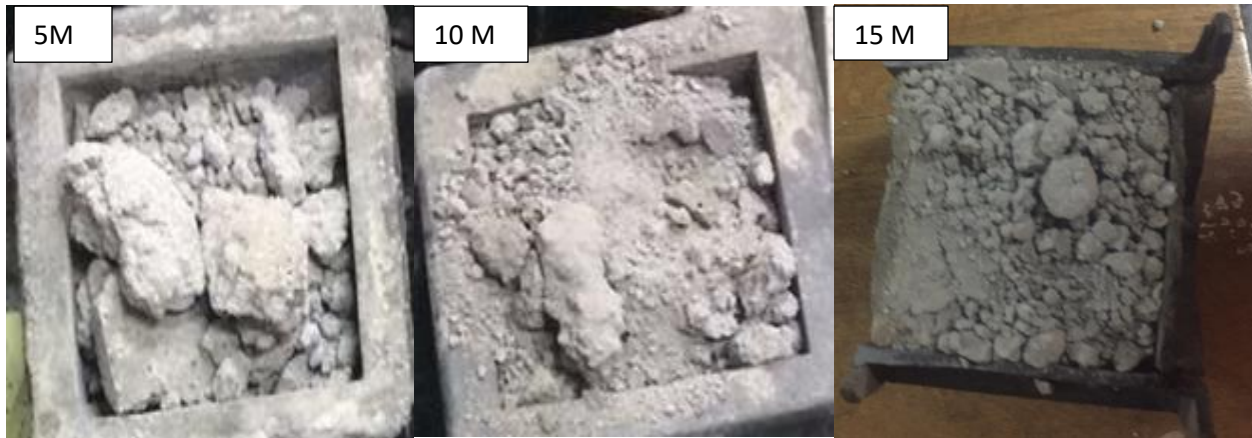
155 **2.6. Water absorption tests**

156 The specimen was immersed in water for 24 h. After 24 h the specimen was removed from water  
157 and wiped with soft cloth. The wet specimen was weighed within 3 minutes of being removed.

158 **3. Results and discussion**

159 **3.1. Effect of using different particle size**

160

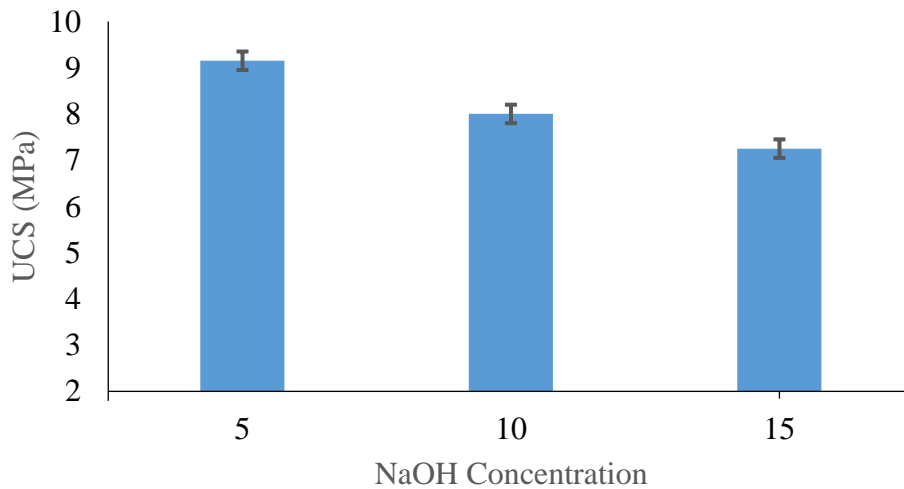


161  
162 **Fig. 1. Picture of casting at different particle size with variation in NaOH concentration**

163 Fig 1 shows the resulting product after attempting to make a geopolymer using different sizes of  
164 BOFS ranging from gravel to sand. The geopolymer did not form, the dried paste crumbled during  
165 demolding process. The BOFS was then milled to a finer particles size, it has been reported by  
166 several authors that uniform particle sizes enhances and increases the mechanical properties of  
167 geopolymer gel (Duxson et al., 2005; Part et al., 2015; Issabella et al., 2003; Ryu et al., 2013).

168

169 **3.2. Effect of NaOH concentration on UCS**



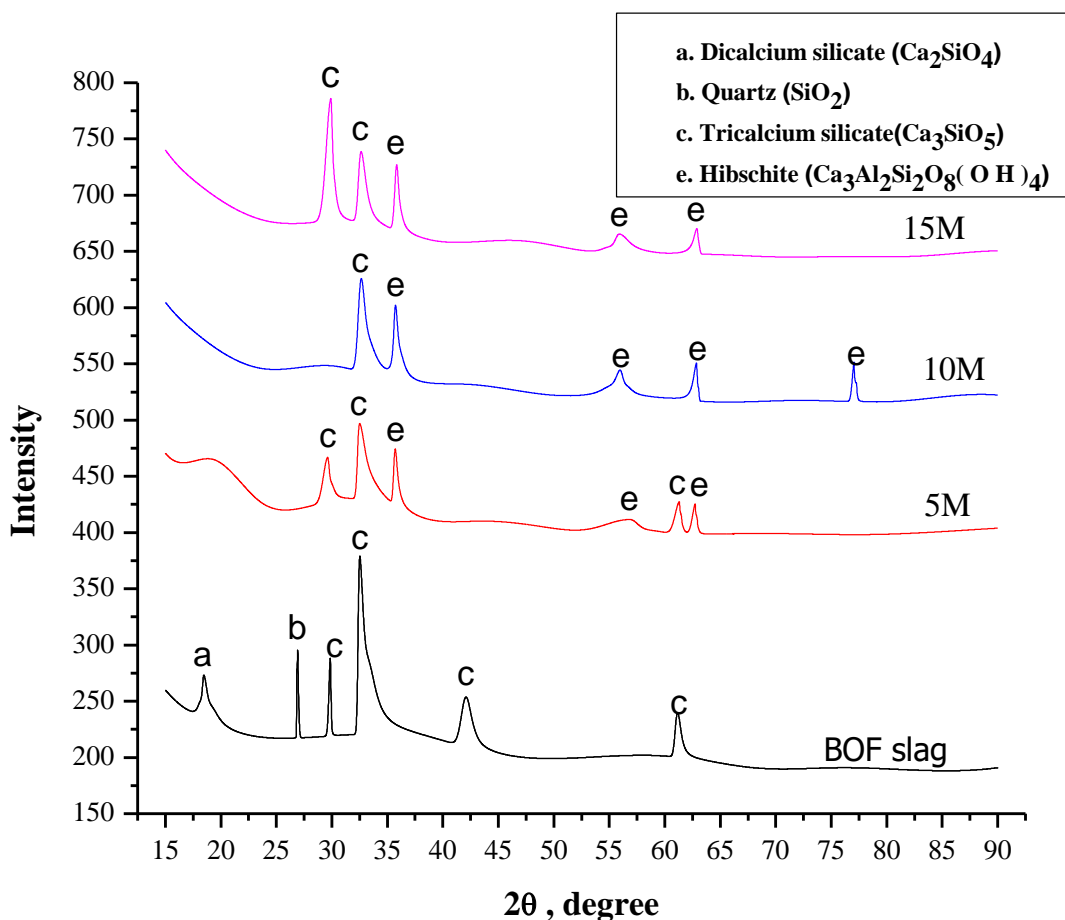
170  
171

**Fig 2. Effect of NaOH concentration on UCS**

172 Fig 2 shows that indeed a uniform particle sizes ranging from 0.425-0.075 micron of BOF slag can  
173 be synthesized a BOF slag based geopolymer with low content of silica to alumina. The highest  
174 strength achieved under NaOH activation is 9.2 MPa. There was a decrease in UCS with increase  
175 in NaOH concentration. This was due to reduced workability of the paste formed. The geopolymer

176 paste hardened faster at 15 M than 5 M and 10 M reducing the time for dissolution of  
 177 aluminosilicate species. It was also observed that as the concentration of NaOH was increased the  
 178 paste tend to be less workable meaning that the paste needed more water to increase the workability  
 179 which might lead to an increase in the UCS.

### 180 3.3. XRD Analysis



181  
 182 **Fig 3 XRD patterns before and after alkaline activation**  
 183 Fig 3 shows the diffractograms of BOF slag before and after geopolymerisation. Upon alkaline  
 184 activation by NaOH (5M, 10M and 15M) the quartz (SiO<sub>2</sub>) peak at 26.9° and dicalcium silicate  
 185 (Ca<sub>2</sub>SiO<sub>4</sub>) at 18.4° disappeared. The disappearance of these peaks show a rapid reactivity of BOF  
 186 slag. The tricalcium silicate was slightly consumed during alkaline activation; as its intensity at  
 187 32.5 decrease with a decrease in NaOH concentration. The high strength at 5 M might be due to  
 188 more tricalcium silicate being consumed and reacting resulting in hardening, initial setting and  
 189 early strength development of BOF slag geopolymeric paste. As the peak intensity of C<sub>3</sub>S, C<sub>2</sub>S



190 and SiO<sub>2</sub> decrease; in parallel a hydrated phase; hibschite is formed. There are more hibschite  
 191 peaks formed at 10 M and 15 M; their peak intensity are even more pronounced as compared to  
 192 those at 5 M. This might be due to excess hydroxide ions concentration which caused the  
 193 geopolymeric gel to precipitate, hindering the poly-condensation process; hence the decrease in  
 194 strength at 15 and 10M. Table 2 shows the quantitative phase amounts from XRD.

195

196

**Table 2: Quantitative phase amount**

	BOF slag	5 M	10 M	15 M
Dicalcium silicate Ca <sub>2</sub> SiO <sub>4</sub>	14.9	2.5	3.8	4.7
Tricalcium silicate (Ca <sub>3</sub> SiO <sub>5</sub> )	14.4	4.6	6.5	7.5
Quartz (SiO <sub>2</sub> )	7.18	0.51	1.56	2.76
Calcium Oxide (CaO)	13.9	3.2	4.4	7.5
Brownmillerite (Ca <sub>2</sub> (Al,Fe) <sub>2</sub> O <sub>5</sub> )	38.3	5.3	7.56	8.6
Hematite Fe <sub>2</sub> O <sub>3</sub>	11.3	2.9	2.7	2.7
Hibschite [Ca <sub>3</sub> Al <sub>3</sub> Si <sub>2</sub> O <sub>8</sub> (OH) <sub>4</sub> ]	0	70.63	77.01	80.2
Zeolite Y, Na (Na <sub>2</sub> Al <sub>2</sub> Si <sub>4.5</sub> O <sub>3</sub> * H <sub>2</sub> O)	0	10.37	1.7	3.8

197

198 Table 2 supports the XRD diffractogram results; that as the concentration of NaOH decrease the  
 199 more the constituents namely; tricalcium silicate, dicalcium silicate, silica and Brownmillerite  
 200 were consumed. The phenomena reveals the reactivity of BOF slag in forming the two zeolites;  
 201 zeolite Y, Na and Hibschite which are responsible for strength development.

202

203

### 204 3.4. SEM analysis

205

206

207

208

209

210

211

212

213

214

215

216

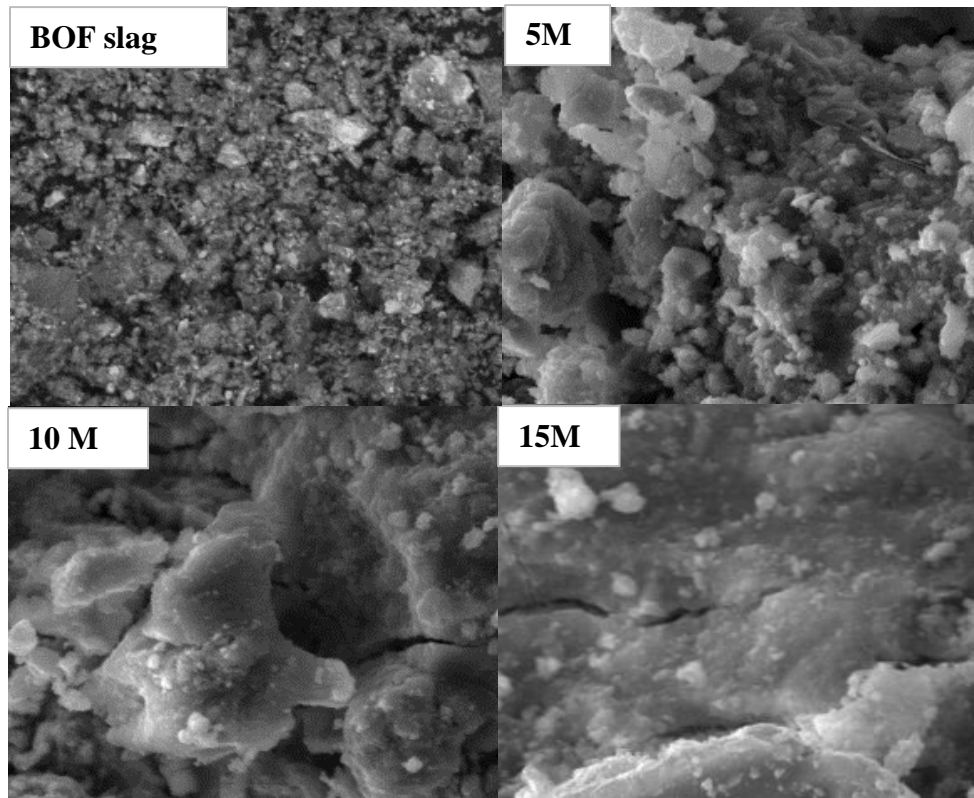
217

218

219

220

221



222

**Fig 4 SEM micrographs before and after alkaline activation**

223 Fig 4 shows the micrographs of BOF slag before and after alkaline activation. Upon alkaline

224 activation the particles appear closed packed flaky and fluffly which reveals that

225 geopolymerisation took place. The 5 M micrograph shows there was formation of a lightly whitish

226 colored particles which represent zeolite structure (Zeolite Y, Na); this is supported by the

227 quantitative analysis using XRD (Falayi et al., 2017). The formation of the zeolite might have been

228 incorporated with the hibschite on the XRD. The increase in strength upon 5 M alkaline activation

229 might be as result of the formation of this zeolite as presence on zeolitic material increases the

230 strength of a geopolymer matrix (Falayi, 2017). The decrease of strength at 10 M and 15 M was a

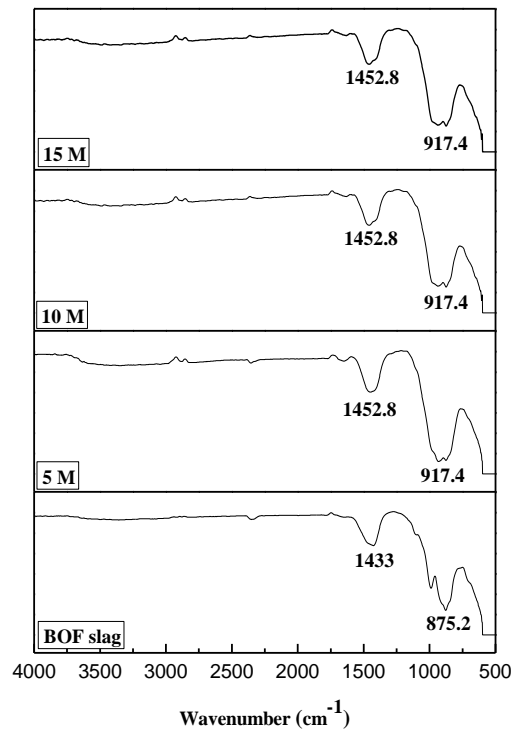
231 result of cracks as shown on the micrographs. Both the cracks are related to the substantial loss of

232 moisture from the geopolymer matrix which resulted in excessive shrinkage during drying and

233 subsequent loss of structural integrity of the BOF slag geopolymer matrix.

234  
235  
236

### 3.5. FTIR analysis



237  
238

**Fig 5 FTIR analysis of BOF slag before and after alkaline activation**

239 Fig. 5. shows the IR bands of BOF slag before and after alkaline activation. The IR spectrum of  
240 BOF slag reveals the main absorption bands at 1433 and 875.2 cm<sup>-1</sup>. The intense band at 875.2  
241 cm<sup>-1</sup> and 1433 cm<sup>-1</sup> are associated with Si–O–Si and Si–O–Al asymmetric stretching vibration.  
242 These intense bands become sharper and move towards higher frequencies of 917.4 cm<sup>-1</sup> and  
243 1452.8 cm<sup>-1</sup> upon alkaline activation (Abdullah et al 2012; Somna et al., 2011). This indicates the  
244 formation of a new product (the aluminosilicate gel phase) due to dissolution of BOF slag in the  
245 alkaline activator.

### 246 3.6. The effect of solid/ liquid on UCS

247

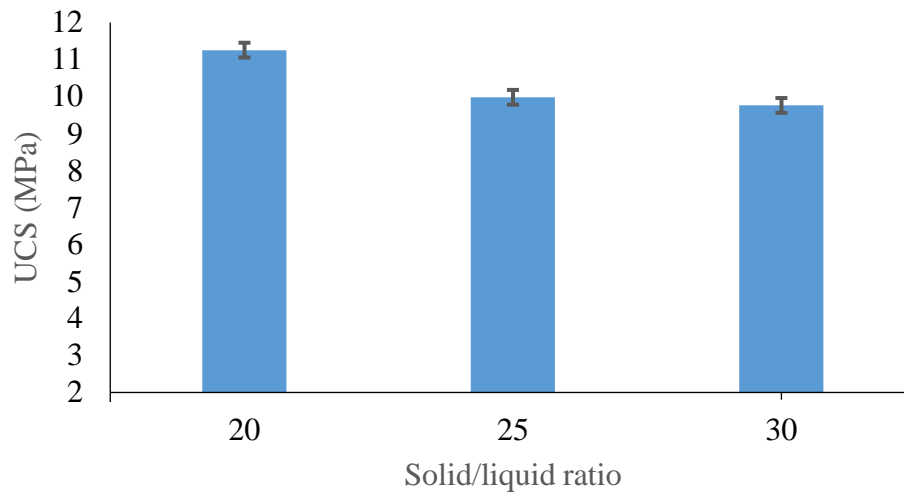


**Fig. 6. The effect of solid to liquid ratio on UCS**

248  
249

250 Fig. 6 shows the UCS of the BOF slag based geopolymer at various S/L ratios with constant  
 251  $\text{Na}_2\text{SiO}_3/\text{NaOH}$  ratio at 2:1. The addition of sodium silicate was to enhance the process of  
 252 geopolymerisation which resulted in 23.3% increase in UCS as compared to when NaOH alone  
 253 was used as the activator (Morsy et al., 2014). There was an increase in UCS with a decrease in  
 254 solid/liquid ratio. The results suggest that the workability of BOF slag based geopolymer decreased  
 255 with increasing S/L ratio. Workability decreased as result of the highly viscous property of sodium  
 256 silicate than the NaOH solution (Heah et al., 2012). By experimental observation at 30 % S/L ratio,  
 257 the geopolymer paste was less workable and exhibits segregation (Suresh and Manojkumar 2013).  
 258 In addition the dried paste appeared peeled off with cracks on one side (see Fig.4.4) which might  
 259 be due to the high amount of activating solution which hinders the geopolymerisation process.  
 260 However, at 25 % S/L ratio, the dried paste had less pronounced cracks as compared to 30 % S/L  
 261 ratio and there was no peeling observed. At 20 % S/L ratio the paste was the most optimum in  
 262 terms of workability and strength, and was thus used to investigate the other variables.

### 263 3.7. The effect of curing temperature

264  
265

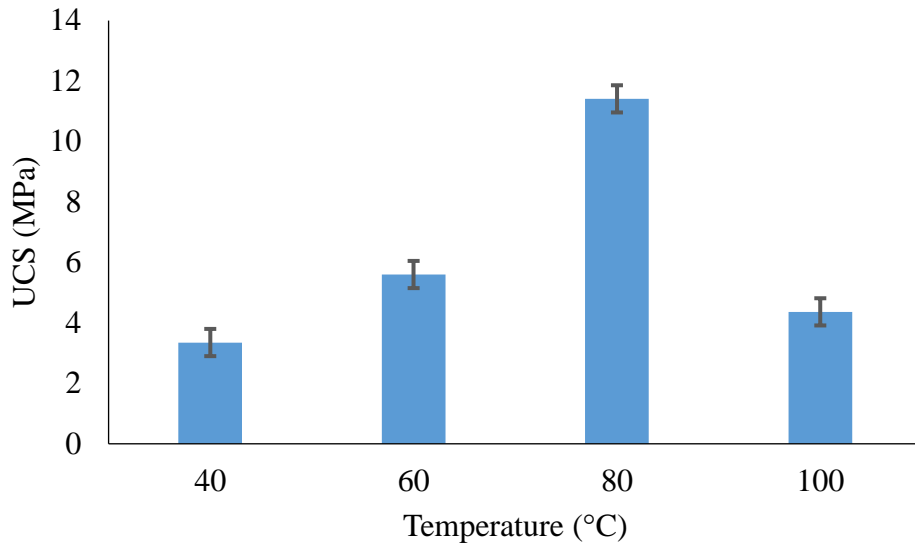


**Fig 8. Effect of temperature on UCS**

266  
267

268 Fig. 8 shows the UCS of the BOF slag based geopolymer at different curing regimes. There was  
 269 an increase in UCS with curing temperature increase from 40°C to 80°C. Basically, the initial  
 270 curing at an elevated temperature (80°C) activates and favors the geopolymerisation process, hence  
 271 there was 70% increase in UCS. An increase in temperature from 80°C to 100°C resulted in (56.7  
 272 %) substantial decrease in UCS. When curing at 100°C, the viscosity increases rapidly at the onset  
 273 of poly-condensation. Therefore, the geopolymer paste hardened faster. This can also be attributed  
 274 to rapid moisture loss at 100°C which results in the paste hardening faster and in turn shortening  
 275 the geopolymerisation process. A similar trend has been reported by (Falayi et al., 2017)

276 **3.8. The effect of Na<sub>2</sub>SiO<sub>3</sub>/NaOH ratio on UCS**  
 277

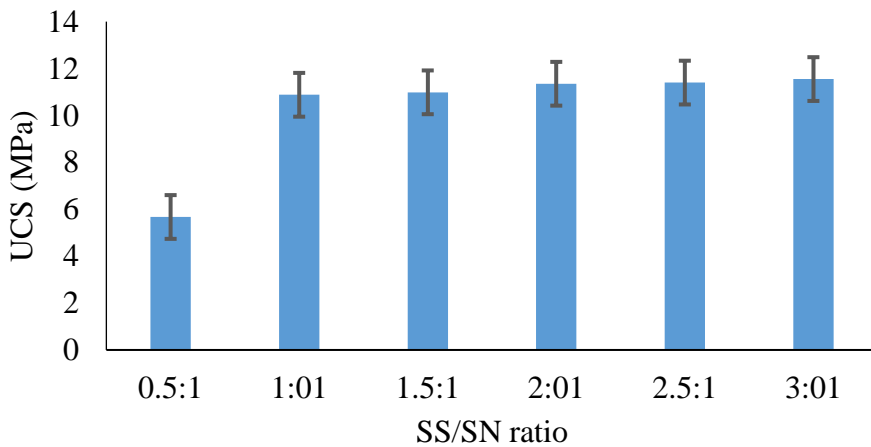


**Fig 9. The effect of S/N ratio on UCS**

278  
279

280 Fig. 9 shows that there was an increase in UCS with increase in  $\text{Na}_2\text{SiO}_3/\text{NaOH}$  (S/N). However,  
 281 the difference in UCS from 1:1 to 3:1 was statistically insignificant as  $F < F_{\text{crit}}$  as shown in Table  
 282 3. The insignificant difference could have resulted from the fact that at 1:1 ratio the dissolution of  
 283 silica and alumina was high leading to improvement in compressive strength of the BOF slag  
 284 geopolymer (Morsy et al., 2014). This reveals that at 1:1 ratio most of the silica and alumina in  
 285 BOF slag are dissolved on the first contact with alkaline activator, accelerating the  
 286 geopolymerisation process, hence thereafter beyond S/N =1:1 the strength was insignificantly  
 287 different. This phenomena consumes the silica and alumina in raw BOF slag material. Basically,  
 288 the increase in the  $\text{Na}_2\text{SiO}_3/\text{NaOH}$  ratio resulted in the increase of sodium content in the mixture.  
 289 Sodium is important for the formation of geopolymers as it acts as charge balancing ions. However,  
 290 excess sodium/ sodium silicate might hinder water evaporation and structure formation; which in  
 291 turn in this case resulted in insignificant difference in the UCS (Škvára et al., 2006). By  
 292 experimental observation the increase in S/N= 1:1 ratio resulted in the geopolymer paste becoming  
 293 very sticky as a result of the viscous nature of the water glass. This resulted in the geopolymer  
 294 hardening faster, hence there was a very slight acceleration of geopolymerisation from 1:1 to 3:1  
 295 ratio which in turn resulted in insignificant change in UCS. The results obtained show that the  
 296 addition of  $\text{Na}_2\text{SiO}_3$  increased the strength of the geopolymer by 23% as compared to when only  
 297 NaOH was used as the activator. This means  $\text{Na}_2\text{SiO}_3$  can be added to the NaOH/BOF slag based  
 298 paste to enhance the geopolymerisation process which; in turn improves the strength of the  
 299 geopolymer.

300 **Table 3 Statistical Anova test**

<i>Source of Variation</i>	<i>SS</i>	<i>df</i>	<i>MS</i>	<i>F</i>	<i>P-value</i>	<i>F crit</i>
Between Groups	0.04096	1	0.04096	0.34535	0.57297	5.31766
Within Groups	0.94884	8	0.11861			
Total	0.9898	9				

301

### 302 **3.9. Wet compressive strength of the LWCB**

303 Table 4 shows the 24 h soak properties of the LWCBs cured under different conditions.

304

305

306  
307  
308

**Table 4: 24 h soak LWCB properties**

BOFS Sample		
Mass of cured sample (kg)	1310	1330
Mass of cured sample after 24hr soak (kg)	1441	1489
UCS before soak (Mpa)	10.4	10.31
UCS after soak (Mpa)	9.496	8.954
% water absorption	10.01	11.95
% reduction in UCS	8.69	13.15
Open porosity	0.131	0.159
Mass after 5 h boil (kg)	1508	1531
Saturation coefficient	0.859	0.794

309

310 The synthesized LWCB cured satisfied the requirements of ASTM C34-13 with an average bulk  
311 density of 1320 kg/m<sup>3</sup>.

#### 312 **4. Conclusions**

313

314 South African BOF slag can be used as a low cost building material. The best geopolymerisation  
315 parameters were obtained at 5 M of NaOH, L/S ratio 20%, SS: SN ratio 1:1 and the curing  
316 temperature 80 °C. The particle size, concentration and quantity of NaOH and curing regime have  
317 a direct effect on the LWCB strength. BOF slag could be alkali activated using NaOH and SS to  
318 produce LWCB that met the minimum requirements for ASTM C34-13, C129-14a and South  
319 African standard (SANS227: 2007). The zeolite Hibschite was responsible for the strength  
320 development of the LWCB. The addition of SS increased the strength of the LWCB by 25% as  
321 compared to when only NaOH is used as the alkaline activator. The BOF slag characterization  
322 revealed that it's a sandy material with non-shrinking behavior and non-expansive as shown in the  
323 wet compressive strength results.

#### 324 **References**

325

326 Abdullah, M.M.A.B., Hussin, K., Bnhussain, M., Ismail, K.N., Yahya, Z. and Abdul Razak, R.,  
327 2012. Fly ash-based geopolymer lightweight concrete using foaming agent. *International Journal*  
328 *of Molecular Sciences*, 13(6), pp.7186-7198.

329 Ameri, M., Hesami, S. and Goli, H., 2013. Laboratory evaluation of warm mix asphalt mixtures  
330 containing electric arc furnace (EAF) steel slag. *Construction and Building materials*, 49, pp.611-  
331 617.

332 Bah, M.M. and Azam, M., 2017. Investigating the relationship between electricity consumption  
333 and economic growth: Evidence from South Africa. *Renewable and Sustainable Energy*  
334 *Reviews*, 80, pp.531-537.

335 Belhadj, E., Diliberto, C. and Lecomte, A., 2014. Properties of hydraulic paste of basic oxygen  
336 furnace slag. *Cement and Concrete Composites*, 45, pp.15-21.

337 Bernard, B., Wang'ombe, D. and Kitindi, E., 2017. Carbon Markets: Have They Worked for  
338 Africa. *Review of Integrative Business and Economics Research*, 6(2), p.90.

339 Brand, A.S. and Roesler, J.R., 2015. Steel furnace slag aggregate expansion and hardened concrete  
340 properties. *Cement and Concrete Composites*, 60, pp.1-9.

341 Chen, J.S. and Wei, S.H., 2016. Engineering properties and performance of asphalt mixtures  
342 incorporating steel slag. *Construction and Building Materials*, 128, pp.148-153.

343 Duxson, P., Provis, J.L., Lukey, G.C., Mallicoat, S.W., Kriven, W.M. and Van Deventer, J.S.,  
344 2005. Understanding the relationship between geopolymer composition, microstructure and  
345 mechanical properties. *Colloids and Surfaces A: Physicochemical and Engineering Aspects*,  
346 269(1), pp.47-58.

347 Egesi, N. and Akaha, C.T., 2012. Engineering-Geological Evaluation of Rock Materials from  
348 Bansara, Bamenda Massif Southeastern Nigeria, as Aggregates for Pavement  
349 Construction. *Geosciences*, 2(5), pp.107-111.

350 Falayi, T., Okonta, F.N. and Ntuli, F., 2017. Desilication of fly ash and development of lightweight  
351 construction blocks from alkaline activated desilicated fly ash. *International Journal of*  
352 *Environment and Waste Management*, 20(3), pp.233-253.



353 Haritonovs, V., Brencis, G., Zaumanis, M. and Smirnovs, J., 2013. Use of Unconventional  
354 Aggregates in Hot Mix Asphalt Concrete. *Construction Science*, 14, pp.44-49.

355 Heah, C.Y., Kamarudin, H., Al Bakri, A.M., Bnhussain, M., Luqman, M., Nizar, I.K., Ruzaidi,  
356 C.M. and Liew, Y.M., 2012. Study on solids-to-liquid and alkaline activator ratios on kaolin-based  
357 geopolymers. *Construction and Building Materials*, 35, pp.912-922.

358 Ioannou, I., Fournari, R. and Petrou, M.F., 2013. Testing the soundness of aggregates using  
359 different methodologies. *Construction and Building Materials*, 40, pp.604-610.

360 Isabella, C., Lukey, G.C., Xu, H. and van Deventer, J.S., 2003. The effect of aggregate particle  
361 size on formation of geopolymeric gel.

362 Kumar, S., Kumar, R. and Mehrotra, S.P., 2010. Influence of granulated blast furnace slag on the  
363 reaction, structure and properties of fly ash based geopolymer. *Journal of Materials Science*, 45(3),  
364 pp.607-615.

365 Motz, H. and Geiseler, J., 2001. Products of steel slags an opportunity to save natural  
366 resources. *Waste Management*, 21(3), pp.285-293.

367 Morsy, M.S., Alsayed, S.H., Al-Salloum, Y. and Almusallam, T., 2014. Effect of sodium silicate  
368 to sodium hydroxide ratios on strength and microstructure of fly ash geopolymer binder. *Arabian*  
369 *Journal for Science and Engineering*, 39(6), pp.4333-4339.

370 Ohanyere, C.I. and Alexander, M.G., 2013. *The South African cement industry: A review of its*  
371 *energy efficiency and environmental performances since 1980* (Doctoral dissertation, University  
372 of Cape Town, Cape Town).

373 Part, W.K., Ramli, M. and Cheah, C.B., 2015. An overview on the influence of various factors on  
374 the properties of geopolymer concrete derived from industrial by-products. *Construction and*  
375 *Building Materials*, 77, pp.370-395.

376 Pelser, W.A., 2017. *A system for continuous energy management to improve cement plant*  
377 *profitability* (Doctoral dissertation, North-West University (South Africa), Potchefstroom  
378 Campus).

379 Pereira, A.P.D.S., Silva, M.H.P.D., Júnior, L., Pereira, É., Paula, A.D.S. and Tommasini, F.J.,  
380 2017. Processing and Characterization of PET Composites Reinforced With Geopolymer Concrete  
381 Waste. *Materials Research*, (AHEAD), pp.0-0.

382 Reddy, A.S., Pradhan, R.K. and Chandra, S., 2006. Utilization of basic oxygen furnace (BOF) slag  
383 in the production of a hydraulic cement binder. *International Journal of Mineral*  
384 *Processing*, 79(2), pp.98-105.

385 Ren, C., Wang, W. and Li, G., 2017. Preparation of high-performance cementitious materials from  
386 industrial solid waste. *Construction and Building Materials*, 152, pp.39-47.

387 Ryu, G.S., Lee, Y.B., Koh, K.T. and Chung, Y.S., 2013. The mechanical properties of fly ash-  
388 based geopolymer concrete with alkaline activators. *Construction and Building Materials*, 47,  
389 pp.409-418.

390 Shen, D.H., Wu, C.M. and Du, J.C., 2009. Laboratory investigation of basic oxygen furnace slag  
391 for substitution of aggregate in porous asphalt mixture. *Construction and Building*  
392 *Materials*, 23(1), pp.453-461.

393 Shi, C., 2002. Characteristics and cementitious properties of ladle slag fines from steel  
394 production. *Cement and Concrete Research*, 32(3), pp.459-462.

395 Škvára, F., Kopecký, L., Nemecek, J. and Bittnar, Z.D.E.N.Ì.K., 2006. Microstructure of  
396 geopolymer materials based on fly ash. *Ceramics-Silikaty*, 50(4), pp.208-215.

397 Somna, K., Jaturapitakkul, C., Kajitvichyanukul, P. and Chindapasirt, P., 2011. NaOH-activated  
398 ground fly ash geopolymer cured at ambient temperature. *Fuel*, 90(6), pp.2118-2124.

399 Suresh, G., Manojkumar, P., 2013. Factors influencing compressive strength of geopolymer  
400 concrete. *International Journal of Research in Engineering and Technology*, 2319-1163, pp. 2321-  
401 7308.

402 Taherkhani, H., 2015. Evaluation of the Physical Properties of Unbound Base Layer Containing  
403 Recycled Aggregates. *International Journal of Environmental Science and Development*, 6(4),  
404 p.279.

405 Tsakiridis, P.E., Papadimitriou, G.D., Tsivilis, S. and Koroneos, C., 2008. Utilization of steel slag  
406 for Portland cement clinker production. *Journal of Hazardous Materials*, 152(2), pp.805-811.

407 Wang, Q. and Yan, P., 2010. Hydration properties of basic oxygen furnace steel slag. *Construction*  
408 *and Building Materials*, 24(7), pp.1134-1140.

409 Xue, Y., Wu, S., Hou, H. and Zha, J., 2006. Experimental investigation of basic oxygen furnace  
410 slag used as aggregate in asphalt mixture. *Journal of Hazardous Materials*, 138(2), pp.261-268.

411 Yildirim, I.Z. and Prezzi, M., 2011. Chemical, mineralogical, and morphological properties of  
412 steel slag. *Advances in Civil Engineering*, 2011.

413 Yildirim, I.Z. and Prezzi, M., 2015. Geotechnical properties of fresh and aged basic oxygen  
414 furnace steel slag. *Journal of Materials in Civil Engineering*, 27(12), p.04015046.

415 Yüksel, İ., 2017. A review of steel slag usage in construction industry for sustainable development.  
416 *Environment, Development and Sustainability*, 19(2), pp.369-384.

417 Zhang, L., Ahmari, S. and Zhang, J., 2011. Synthesis and characterization of fly ash modified mine  
418 tailings-based geopolymers. *Construction and Building Materials*, 25(9), pp.3773-3781.

419

420